



Article

# Heterologous Expression of Nitrate Assimilation Related-Protein DsNAR2.1/NRT3.1 Affects Uptake of Nitrate and Ammonium in Nitrogen-Starved *Arabidopsis*

Hongping Ma<sup>1</sup>, Junchao Zhao<sup>1</sup>, Shuang Feng<sup>2,3</sup>, Kun Qiao<sup>1</sup>, Shufang Gong<sup>1</sup>, Jingang Wang<sup>1,\*</sup> and Aimin Zhou<sup>1,\*</sup> 

<sup>1</sup> College of Horticulture and Landscape Architecture, Northeast Agricultural University, Harbin 150030, China; HongpingMa@aliyun.com (H.M.); ZhaoJunchaos@outlook.com (J.Z.); kunqiao@neau.edu.cn (K.Q.); shufanggong@neau.edu.cn (S.G.)

<sup>2</sup> Key Laboratory of Saline-Alkali Vegetation Ecology Restoration (Northeast Forestry University), Ministry of Education, Harbin 150040, China; shuangfeng1986@aliyun.com

<sup>3</sup> College of Life Sciences, Northeast Forestry University, Harbin 150040, China

\* Correspondence: wangjingang99@neau.edu.cn (J.W.); aiminzhou@neau.edu.cn (A.Z.); Tel.: +86-451-5519-0743 (J.W. & A.Z.)

Received: 5 May 2020; Accepted: 2 June 2020; Published: 4 June 2020



**Abstract:** Nitrogen (N) is an essential macronutrient for plant growth. Plants absorb and utilize N mainly in the form of nitrate ( $\text{NO}_3^-$ ) or ammonium ( $\text{NH}_4^+$ ). In this study, the nitrate transporter DsNRT3.1 (also known as the nitrate assimilation-related protein DsNAR2.1) was characterized from *Dianthus spiculifolius*. A quantitative PCR (qPCR) analysis showed that the *DsNRT3.1* expression was induced by  $\text{NO}_3^-$ . Under N-starvation conditions, the transformed *Arabidopsis* seedlings expressing *DsNRT3.1* had longer roots and a greater fresh weight than the wild type. Subcellular localization showed that DsNRT3.1 was mainly localized to the plasma membrane in *Arabidopsis* root hair cells. Non-invasive micro-test (NMT) monitoring showed that the root hairs of N-starved transformed *Arabidopsis* seedlings had a stronger  $\text{NO}_3^-$  and  $\text{NH}_4^+$  influx than the wild-type seedlings, using with  $\text{NO}_3^-$  or  $\text{NH}_4^+$  as the sole N source; contrastingly, transformed seedlings only had a stronger  $\text{NO}_3^-$  influx when  $\text{NO}_3^-$  and  $\text{NH}_4^+$  were present simultaneously. In addition, the qPCR analysis showed that the expression of *AtNRT2* genes (*AtNRT2.1–2.6*), and particularly of *AtNRT2.5*, in the transformed *Arabidopsis* differed from that in the wild type. Overall, our results suggest that the heterologous expression of *DsNRT3.1* affects seedlings' growth by enhancing the  $\text{NO}_3^-$  and  $\text{NH}_4^+$  uptake in N-starved *Arabidopsis*. This may be related to the differential expression of *AtNRT2* genes.

**Keywords:** nitrogen; *DsNRT3.1*; heterologous expression;  $\text{NO}_3^-$  and  $\text{NH}_4^+$  uptake; seedling growth; *Arabidopsis*

## 1. Introduction

Nitrogen (N) is an essential macronutrient for plant growth and crop productivity [1]. Plants acquire inorganic N from the soil, mainly in the form of nitrate ( $\text{NO}_3^-$ ) and ammonium ( $\text{NH}_4^+$ ) [2]. Under aerobic conditions,  $\text{NO}_3^-$  is usually the most abundant N source in soil, and it is the predominant form of N absorbed by most plants [3]. For some species, such as rice (*Oryza sativa*) and *Camellia sinensis*,  $\text{NH}_4^+$  is the preferred N source [4,5]. The  $\text{NO}_3^-$  uptake system in higher plants includes a low-affinity transport system (LATS) and a high-affinity transport system (HATS) to accommodate changes in  $\text{NO}_3^-$  concentrations in the soil [6].

The root uptake of  $\text{NO}_3^-$  and transport to the whole plant are regulated by  $\text{NO}_3^-$  transporters (NRTs) [6,7]. NRTs consists of three gene families, *NRT1* (also named NPF, nitrate transporter 1 (NRT1)/peptide transporter (PTR) gene family), *NRT2*, and *NRT3* (also named NAR, nitrate assimilation-related protein) [3]. The NRT1 family comprises many genes—53 members in *Arabidopsis* and 93 members in the rice genome [8,9]. It is suggested that most members of the NRT1 family function as the main components of the LATS at high concentrations of  $\text{NO}_3^-$  [6]. Under low  $\text{NO}_3^-$  concentrations, NRT2 and NRT3/NAR families can function as the major components of the HATS for the root  $\text{NO}_3^-$  influx [6,7,10]. The NRT2 family has seven members (AtNRT2.1–2.7) in *Arabidopsis* [11], and five members (OsNRT2.1, 2.2, 2.3a, 2.3b, and OsNRT2.4) in the rice genome [12]. The many members of the NRT2 family are unable to transport  $\text{NO}_3^-$  alone; they require a partner protein, NRT3/NAR2. The first NRT3/NAR2 gene was identified in *Chlamydomonas reinhardtii*; it functions with CrNRT2 members in the  $\text{NO}_3^-$  influx [13]. In both *Arabidopsis* and rice, the NRT3/NAR2 families have two members, AtNRT3.1 and AtNRT3.2 and OsNAR2.1 and OsNAR2.2 [10–12]. *Arabidopsis* NRT2 members (AtNRT2.1–2.6) require AtNRT3.1 for  $\text{NO}_3^-$  uptake [14,15]. In *atnrt 3.1* mutant plants, the high-affinity  $\text{NO}_3^-$ -inducible influx was reduced [16]. Except for AtNRT2.7, the other six AtNRT2 transporters interact with AtNRT3.1 [15]. Furthermore, the plasma membrane complex of AtNRT3.1 and AtNRT2.5 has been found to be a major contributor to constitutive high-affinity  $\text{NO}_3^-$  influx in *Arabidopsis* [17]. Similarly, the rice OsNRT2 members (OsNRT2.1, 2.2 and 2.3a) require OsNAR2.1 for their  $\text{NO}_3^-$  uptake [12,18]. Both high- and low-affinity  $\text{NO}_3^-$  transport were greatly impaired by OsNAR2.1 knockdown. Yeast two hybrid screening showed that OsNAR2.1 interacted with OsNRT2.1, OsNRT2.2, and OsNRT2.3a [18]. Furthermore, the arginine 100 and aspartic acid 109 of OsNAR2.1 were found to be key amino acids in their interaction with OsNRT2.3a, and their interaction occurs in the plasma membrane [19]. These studies demonstrate that NRT3 is essential for high-affinity NRT2 in  $\text{NO}_3^-$  uptake in *Arabidopsis* and rice.

*Dianthus spiculifolius* Schur (Caryophyllaceae), a perennial herbaceous flowering plant, is a high-economic value ornamental crop with a high economic value that has strong resistance to cold, drought, and barren conditions. Studying its tolerance toward barren soil contributes to expanding its application and production in barren soils. The NRT genes play key roles in N absorption and utilization by plants. In this study, the *DsNRT3.1* gene was identified from the transcriptome of *D. spiculifolius* [20]. Its expression in response to different N sources was investigated using qPCR. The subcellular localization of *DsNRT3.1* in plant cells was observed using green fluorescent protein (GFP) as a marker. We compared the phenotypes of the transformed *Arabidopsis* seedlings expressing *DsNRT3.1* and wild-type seedlings with different N sources ( $\text{NO}_3^-$  or  $\text{NH}_4^+$ ). We monitored the net fluxes of  $\text{NO}_3^-$  and  $\text{NH}_4^+$  in transformed *Arabidopsis* root hairs with different N sources using non-invasive micro-test (NMT) technology.

## 2. Results

### 2.1. Expression Analysis of *DsNRT3.1*

The complete cDNA sequence of *DsNRT3.1* was isolated from the *D. spiculifolius* transcriptome, which contains a 585 bp open reading frame that encodes 194 amino acids and has a predicted molecular mass of 21.07 kDa. The sequence and phylogenetic tree analysis revealed that the *DsNRT3.1* protein was similar to AtNRT3.1 (42.86% amino acid sequence identity) and NRT3.1 from *Arabidopsis* and other species (Figure 1A,B). Two transmembrane domains of the *DsNRT3.1* protein were predicted using HMMTOP software (Figure 1C).

The expression of *DsNRT3.1* in seedlings supplied with different N sources was investigated. The qPCR analysis revealed that the addition of exogenous  $\text{KNO}_3$  (1 mM), KCl (1 mM), or  $\text{NH}_4\text{NO}_3$  (1 mM) significantly induced the *DsNRT3.1* expression (Figure 2A,B). By 3 h of treatment,  $\text{KNO}_3$  and KCl induced the upregulation of *DsNRT3.1* expression by six-fold and two-fold, respectively. By 6–24 h, both  $\text{KNO}_3$  and KCl induced the upregulation of *DsNRT3.1* expression by 4–6-fold. By 3–24 h, the

addition of  $\text{NH}_4\text{NO}_3$  (1 mM) induced the upregulation of *DsNRT3.1* expression by 4–8-fold. However,  $(\text{NH}_4)_2\text{SO}_4$  (0.5 mM) did not significantly affect the *DsNRT3.1* expression (Figure 2B). This indicates that the *DsNRT3.1* expression was affected by  $\text{NO}_3^-$  and  $\text{K}^+$ .

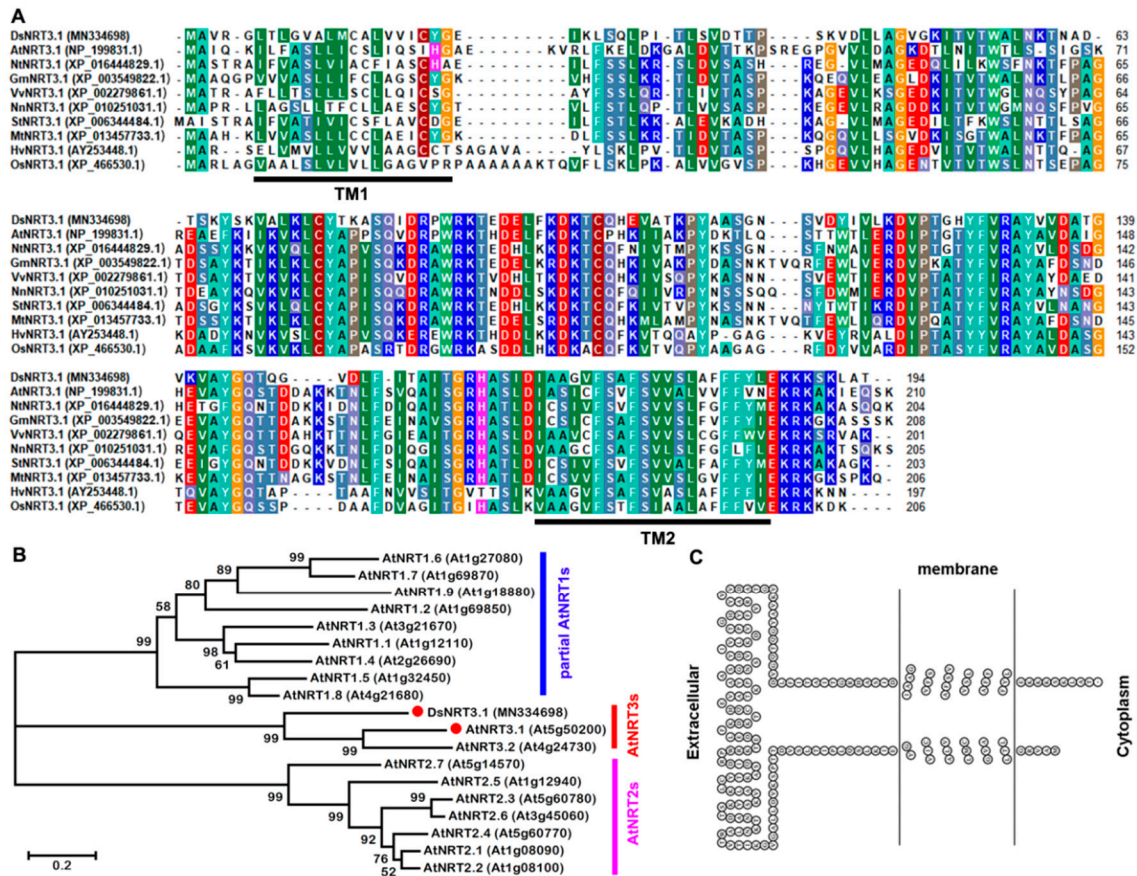


**Figure 1.** Sequence analysis of *DsNRT3.1*. (A) Amino acid sequence alignment of *NRT3.1* from multiple plant species. The black lines indicate the positions of the two transmembrane (TM) domains. (B) Phylogenetic tree of *DsNRT3.1* with *NRT* family members (*AtNRT1*, *AtNRT2*, and *AtNRT3*) from *Arabidopsis*. (C) Transmembrane domain prediction of *DsNRT3.1*.

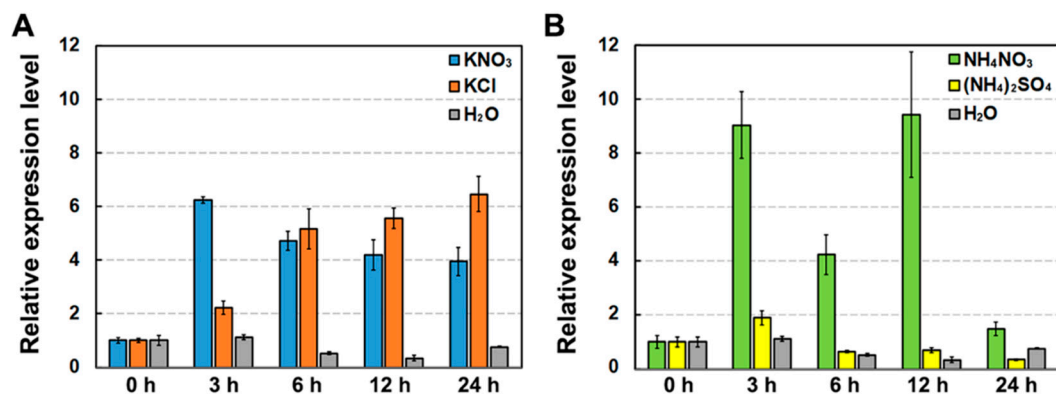


**Figure 2.** Effects of nitrate and ammonium nitrogen on the *DsNRT3.1* gene expression. One-week-old *D. spiculifolius* seedlings were transferred to a  $\text{H}_2\text{O}$  solution (negative control), a  $\text{H}_2\text{O}$  solution containing 1 mM of  $\text{KNO}_3$  or 1 mM of  $\text{KCl}$  (A), or a  $\text{H}_2\text{O}$  solution containing 1 mM of  $\text{NH}_4\text{NO}_3$  or 0.5 mM of  $(\text{NH}_4)_2\text{SO}_4$  (B) treated for 0, 3, 6, 12, and 24 h. *DsActin* was used as an internal reference. Error bars represent the standard error ( $n = 3$ ).

## 2.2. Effect of Heterologous Expression of *DsNRT3.1* on *Arabidopsis* Seedlings Growth

Transformed *Arabidopsis* seedlings expressing *DsNRT3.1*, generated using the 35S promoter, were used to investigate the role of *DsNRT3.1* in plant growth. The expression of *DsNRT3.1* in the transformed *Arabidopsis* lines was confirmed using a semi-quantitative RT-PCR (Figure 3A). After 10 days on N-free 1/2 strength Murashige and Skoog (MS) medium, wild-type and transformed seedlings showed the N-starvation phenotype, but there was no significant difference in the primary root length. On N-free 1/2 MS medium supplemented with  $\text{NO}_3^-$  or  $\text{NH}_4^+$  (0.01 or 0.02 mM) as the sole N source, the primary roots of the transformed seedlings were significantly longer than those of the wild-type seedlings. At  $\text{NO}_3^-$  or  $\text{NH}_4^+$  concentrations over 1 mM, there was no significant difference in primary root length between the wild-type and transformed seedlings (Figure 3B–D). Furthermore, the fresh weight of the transformed seedlings was generally higher than that of the wild-type seedlings after 20 days on N-free 1/2 MS medium supplemented with  $\text{NO}_3^-$  (0.05 to 0.5 mM) or  $\text{NH}_4^+$  (0.1 mM) (Figure 4A–C). These results show that with low-concentration  $\text{NO}_3^-$  or  $\text{NH}_4^+$  as the sole N source, the transformed seedlings grew better than the wild-type seedlings.

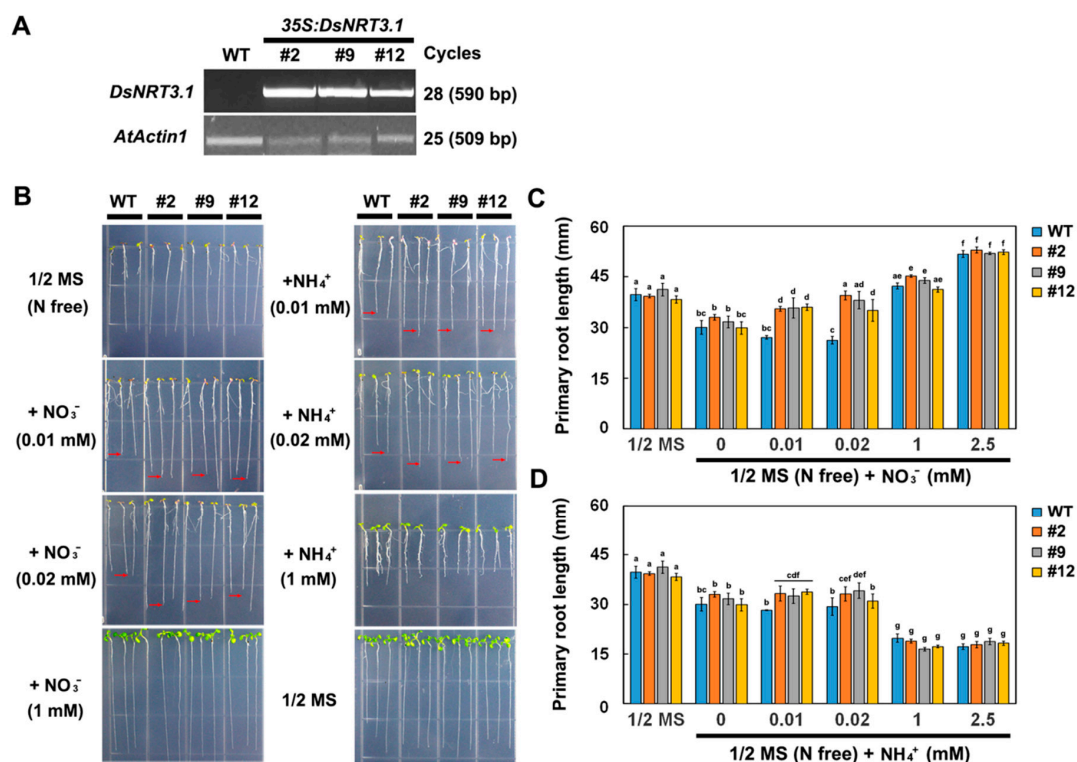


**Figure 3.** Comparison of the seedling root growth of wild-type (WT) and transformed *Arabidopsis* at different N supply levels. **(A)** Semi-quantitative RT-PCR analysis of the *DsNRT3.1* expression in WT and transformed *Arabidopsis* lines (#2, #9, and #12). Phenotype **(B)** and root length **(C,D)** of WT and transformed seedlings grown on 1/2 Murashige and Skoog (MS) medium or N-free 1/2 MS medium supplemented with different concentrations (0, 0.01, 0.02, 1, and 2.5 mM) of  $\text{KNO}_3$  or  $\text{NH}_4\text{Cl}$  for 10 days. Different letters indicate significant differences (Student's *t*-test;  $p < 0.05$ ). Error bars represent the standard error ( $n = 6$ ).

## 2.3. Effect of Heterologous Expression of *DsNRT3.1* on the $\text{NO}_3^-$ and $\text{NH}_4^+$ Fluxes in *Arabidopsis* Root Hairs

It is thought that *DsNRT3.1* is a membrane protein (Figure 1C); therefore, we examined the *DsNRT3.1* localization in *Arabidopsis* using GFP as a marker. In the root hair cells of *Arabidopsis* stably expressing *DsNRT3.1*-GFP, the *DsNRT3.1*-GFP signals were localized mainly to the cell periphery, which is similar to the plasma membrane. However, as a control, the GFP signal was generally distributed throughout the root hair cells of *Arabidopsis* stably expressing GFP (Figure 5A). Root hairs

are a primary site for nutrient uptake in plants [21]. The net  $\text{NO}_3^-$  and  $\text{NH}_4^+$  fluxes in the root hairs of wild-type and transformed *Arabidopsis* were monitored and compared using NMT (Figure 5B).

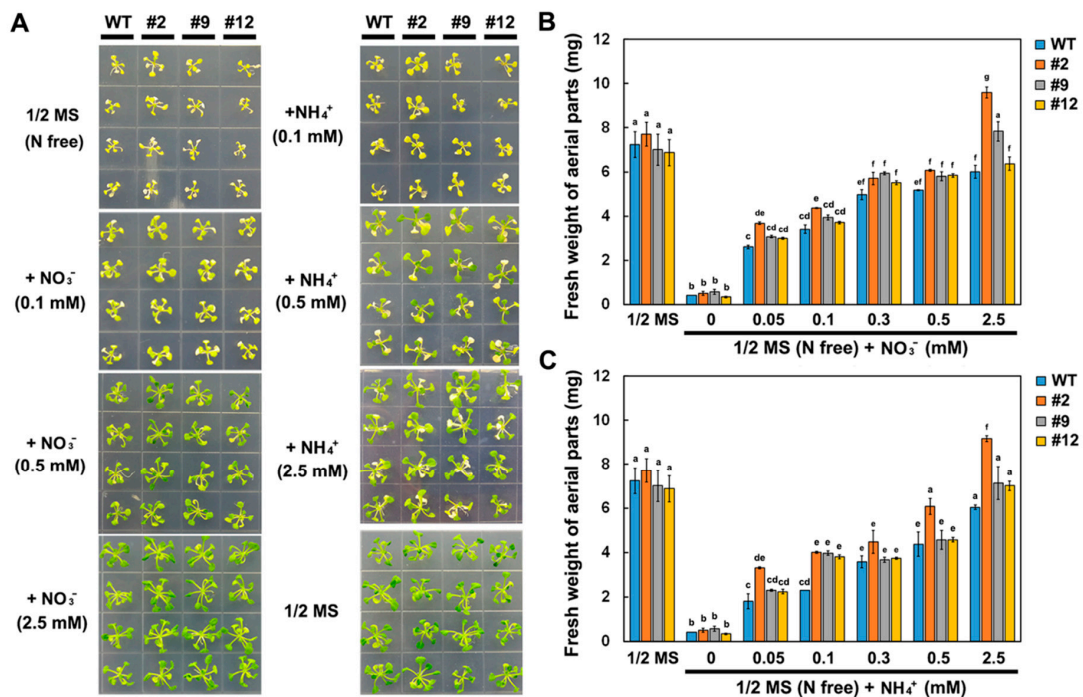


**Figure 4.** Comparison of seedling fresh weight of wild-type (WT) and transformed *Arabidopsis* at different N supply levels. Phenotype (A) and fresh weight (B,C) of WT and transformed seedlings grown on 1/2 MS medium or N-free 1/2 MS medium supplemented with different concentrations (0, 0.05, 0.1, 0.3, 0.5, and 2.5 mM) of  $\text{KNO}_3$  or  $\text{NH}_4\text{Cl}$  for 20 days. Different letters indicate significant differences (Student's *t*-test;  $p < 0.05$ ). Error bars represent the standard error ( $n = 6$ ).

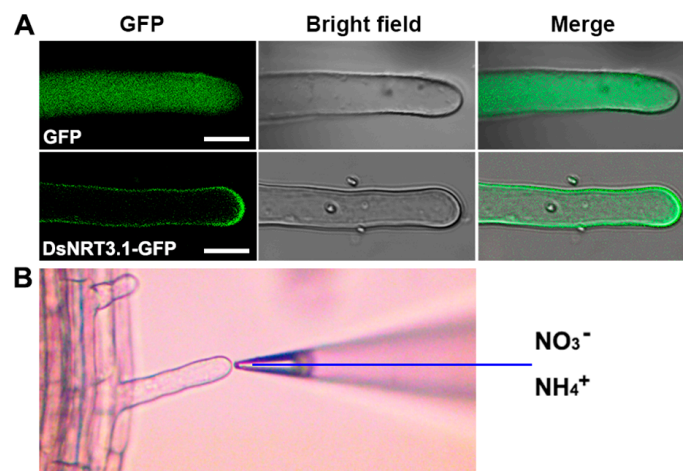


**Figure 5.** Subcellular localization of DsNRT3.1-green fluorescent protein (GFP) in *Arabidopsis* root hair cells. (A) Confocal images of an *Arabidopsis* root hair cell stably expressing GFP or DsNRT3.1-GFP. GFP fluorescence is green. Merged images were created by merging the GFP and bright field images. Scale bars = 10  $\mu\text{m}$ . (B) Morphology and root hair cell sites were monitored using a non-invasive micro-test (NMT). Ion ( $\text{NO}_3^-$  or  $\text{NH}_4^+$ ) selective microelectrodes were used. The monitoring distances were 0 and 20  $\mu\text{m}$  from the end of the root hair cells. The ion flux rate, based on the voltages monitored between two points (0 and 20  $\mu\text{m}$ ), was calculated using iFluxes/imFluxes 1.0 software (Younger USA LLC, Amherst, MA, USA).

Seedlings grown on the 1/2 MS medium or N-free 1/2 MS medium (N-starvation treatment) for 10 days were transferred to a test solution containing  $\text{KNO}_3$  (0.1 mM),  $\text{NH}_4\text{Cl}$  (0.1 mM), or  $\text{NO}_3\text{NH}_4$  (0.5 mM) as the sole N source. With  $\text{KNO}_3$  or  $\text{NH}_4\text{Cl}$  as the sole N source, the root hairs of the wild-type and transformed seedlings cultured on the 1/2 MS medium displayed a marked  $\text{NO}_3^-$  or  $\text{NH}_4^+$  efflux, with no significant difference in the efflux rates between the transformed and wild-type seedlings (Figure 6A–D). However, there was marked  $\text{NO}_3^-$  or  $\text{NH}_4^+$  influx displayed in the root hairs of the N-starved wild-type and transformed seedlings (Figure 6E,G); the mean influx rate in the transformed seedlings was significantly higher than in the wild-type seedlings (Figure 6F,H).

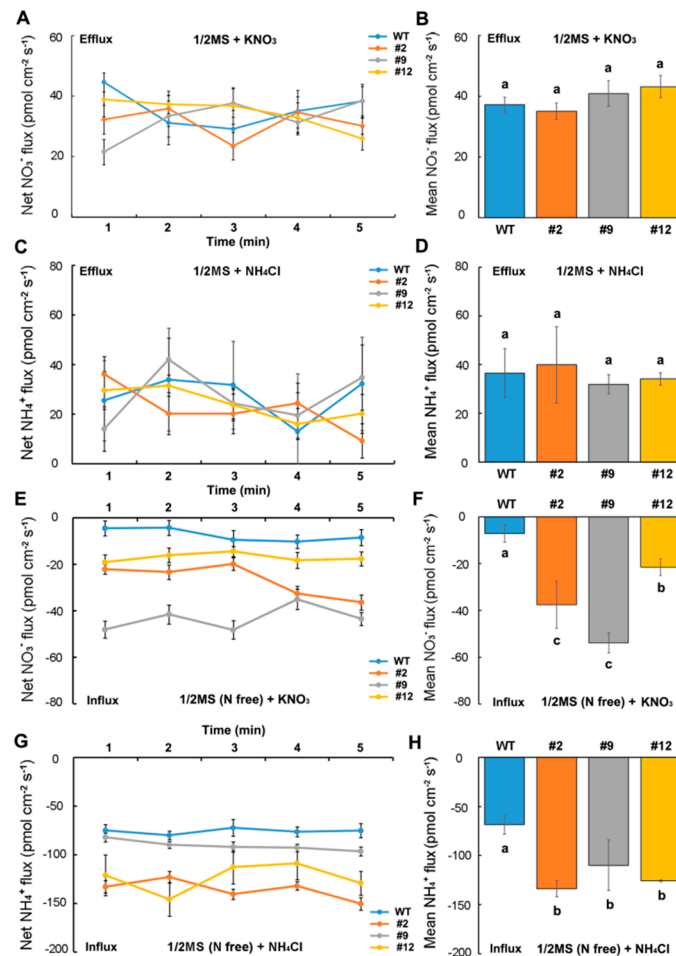


**Figure 6.**  $\text{NO}_3^-$  and  $\text{NH}_4^+$  flux rates in the root hairs of wild-type (WT) and transformed *Arabidopsis* supplied with  $\text{KNO}_3$  or  $\text{NH}_4\text{Cl}$  as the sole N source. WT and transformed seedlings were grown on 1/2 MS medium or N-free 1/2 MS medium for 10 days and transferred to a test solution containing 0.1 mM  $\text{KNO}_3$  or  $\text{NH}_4\text{Cl}$  for 10 min. Then, the net  $\text{NO}_3^-$  and  $\text{NH}_4^+$  fluxes were monitored. Net and mean  $\text{NO}_3^-$  (A,B) or  $\text{NH}_4^+$  (C,D) flux rates of the WT and transformed seedlings grown on the 1/2 MS medium. Net and mean  $\text{NO}_3^-$  (E,F) or  $\text{NH}_4^+$  (G,H) flux rates of the WT and transformed seedlings grown on the N-free 1/2 MS medium. Mean  $\text{NO}_3^-$  (B,F) or  $\text{NH}_4^+$  (D,H) flux rates of six samples ( $n = 6$ ). Different letters indicate significant differences among the transformed lines and WT seedlings (Student's *t*-test;  $p < 0.05$ ). Error bars represent the standard error.

With  $\text{NO}_3\text{NH}_4$  as the sole N source, the root hairs of N-starved transformed seedlings showed a higher  $\text{NO}_3^-$  influx rate than those of the wild type (Figure 7E,F), whereas the  $\text{NH}_4^+$  influx rate was similar to that of the wild type (Figure 7G,H). Moreover, the  $\text{NO}_3^-$  and  $\text{NH}_4^+$  efflux from the root hairs of the wild-type or transformed seedlings cultured on 1/2 MS medium was not marked and showed no significant difference among the lines (Figure 7A–D). This indicates that the root hairs of N-starved

transformed seedlings have a stronger  $\text{NO}_3^-$  uptake ability than those of wild-type seedlings; they also have a stronger  $\text{NH}_4^+$  uptake ability in the absence of  $\text{NO}_3^-$ , suggesting that the heterologous expression of *DsNRT3.1* affects the  $\text{NO}_3^-$  and  $\text{NH}_4^+$  uptake in N-starved *Arabidopsis* seedlings.

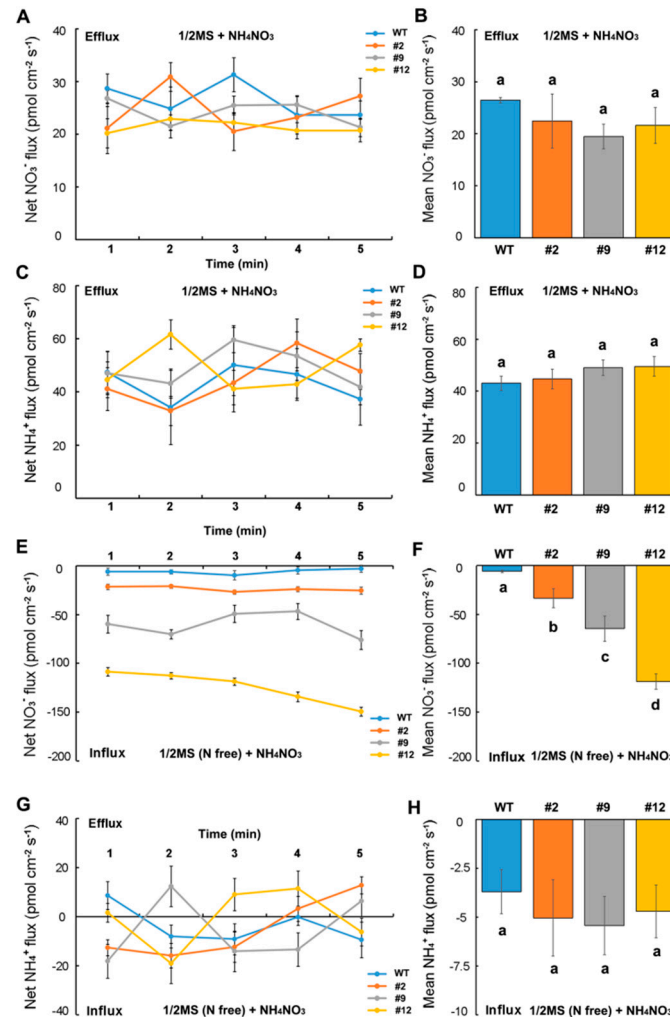


**Figure 7.**  $\text{NO}_3^-$  and  $\text{NH}_4^+$  flux rates in the root hairs of wild-type (WT) and transformed *Arabidopsis* with  $\text{NO}_3\text{NH}_4$  as the sole N source. The WT and transformed seedlings grown on 1/2 MS medium or N-free 1/2 MS medium for 10 d were transferred to a test solution containing 0.1 mM  $\text{NO}_3\text{NH}_4$  for 10 min, and the net  $\text{NO}_3^-$  or  $\text{NH}_4^+$  flux was monitored. Net and mean  $\text{NO}_3^-$  (A,B) or  $\text{NH}_4^+$  (C,D) flux rates of the WT and transformed seedlings grown on the 1/2 MS medium. Net and mean  $\text{NO}_3^-$  (E,F) or  $\text{NH}_4^+$  (G,H) flux rates of the WT and transformed seedlings grown on the N-free 1/2 MS medium. Mean  $\text{NO}_3^-$  (B,F) or  $\text{NH}_4^+$  (D,H) flux rates of six samples ( $n = 6$ ). Different letters indicate significant differences among the transformed lines and WT seedlings (Student's  $t$ -test;  $p < 0.05$ ). Error bars represent the standard error.

#### 2.4. Effect of Heterologous Expression of *DsNRT3.1* on *Arabidopsis* *NRT2* Genes Expression

*NRT3*, as a partner protein to the *NTR2* family, is important for *NRT2* function [15]. The expression levels of *AtNRT2* genes in the wild-type and transformed *Arabidopsis* seedlings were compared. The qPCR analysis revealed that the expression levels of six of the seven *NRT2* family members differed between the transformed *Arabidopsis* and wild-type seedlings; *NRT2.1*, *2.2*, *2.4*, and *2.6* were down-regulated and *NRT2.5* was up-regulated. However, the expression of *AtNRT3.1* and *AtNRT2.7* in transformed *Arabidopsis* was similar to that in the wild type, with no significant difference (Figure 8).

This suggests that the heterologous expression of *DsNRT3.1* affects the expression of members of the *AtNRT2* gene family in transformed *Arabidopsis* seedlings.

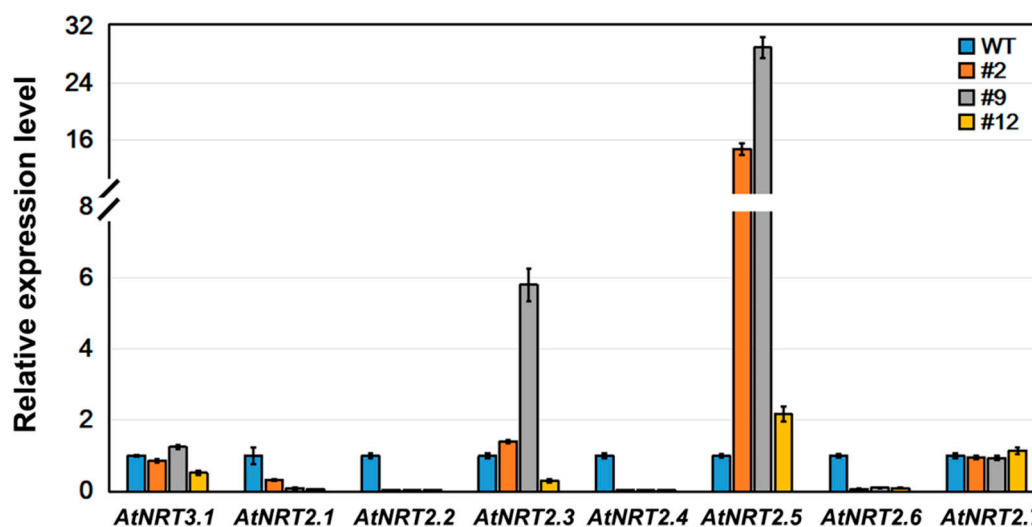


**Figure 8.** Expression analysis of *AtNRT3.1* and *AtNRT2* gene families in wild-type and transformed *Arabidopsis*. *AtActin2* was used as an internal reference. The transcript level of wild-type (WT) seedlings was set at 1.0. Error bars represent the standard error ( $n = 3$ ).

### 3. Discussion

The first NRT3.1 was identified from *Chlamydomonas* [13], and its orthologous proteins were subsequently identified in barley (*HvNRT3.1/HvNAR2.1*) [22], *Arabidopsis* (*AtNRT3.1*) [16], rice (*OsNRT3.1/OsNAR2.1*) [18], and chrysanthemums (*CmNRT3/CmNAR2*) [23]. A sequence analysis showed that *DsNRT3.1* was highly similar to *AtNRT3.1*, *HvNRT3.1*, and *OsNRT3.1/OsNAR2.1* (Figure 1A,B). NRT3.1 was considered to be a high-affinity transporter; it was induced at low concentrations of N sources, whereas its expression was largely unaffected at high concentrations or using saturated N sources. Therefore, we performed a gene expression analysis after N-starvation. In N-starved seedlings, *DsNRT3.1* was also induced by  $\text{NO}_3^-$  (Figure 2). Similarly, the expression of *AtNRT3.1*, *OsNRT3.1/OsNAR2.1*, and *CmNRT3/CmNAR2* was also induced by  $\text{NO}_3^-$  in N-starved seedlings [16,18,23]. However, the expression of *OsNRT3.1/OsNAR2.1* was almost unaffected by  $\text{NH}_4^+$  [18]. We found that *DsNRT3.1* expression was not induced by  $\text{NH}_4^+$  (Figure 2B). In addition,  $\text{K}^+$  affected the *DsNRT3.1* expression (Figure 2A). NRT1.5 from the NRT family serves as a proton-coupled  $\text{H}^+/\text{K}^+$  antiporter for  $\text{K}^+$  loading in *Arabidopsis* [24].

The roots of N-starved transformed *DsNRT3.1* seedlings were longer than those of the wild type under low N conditions, with  $\text{NO}_3^-$  or  $\text{NH}_4^+$  as the sole N source (Figure 3). After longer periods of culture, the fresh weight of the transformed *DsNRT3.1* seedlings was generally higher than that of the wild type (Figure 4). With  $\text{KNO}_3$  as the sole N source, the transformed seedlings had longer roots and higher root  $\text{NO}_3^-$  influx rates than the wild type (Figures 3C and 6E,F). Likewise, with  $\text{NH}_4\text{NO}_3$  as the sole N source, the transformed seedling roots had higher  $\text{NO}_3^-$  influx rates than the wild type (Figure 7E,F). These results suggest that longer root growth in transformed seedlings may be associated with a stronger  $\text{NO}_3^-$  uptake. A confocal observation using GFP as a marker revealed that *DsNRT3.1* was mainly localized to the plasma membrane in *Arabidopsis* root hair cells (Figure 5A). Furthermore, NMT monitoring showed that the root hairs of N-starved transformed seedlings had a stronger  $\text{NO}_3^-$  and  $\text{NH}_4^+$  influx than those of the wild-type seedlings (Figure 6A–D). Several studies have shown that NRT3.1 regulates  $\text{NO}_3^-$  uptake via interaction with NRT2 members on the plasma membrane [15,18,19,23]. Thus, we hypothesized that the heterologous expression of *DsNRT3.1* might affect the  $\text{NO}_3^-$  uptake in N-starved seedlings via interaction with *AtNRT2* members

on the plasma membrane. We compared the expression levels of *AtNRT2* genes in the transformed and wild-type seedlings. The qPCR analysis revealed that the expression of multiple *NRT2* members (*AtNRT2.1–2.6*), and particularly of *AtNRT2.5*, was altered in transformed *Arabidopsis*-expressing *DsNRT3.1* (Figure 8). *Arabidopsis AtNRT2.5* is a high-affinity  $\text{NO}_3^-$  transporter localized on the plasma membrane and is expressed in the root hair zone [25]. Under long-term N-starvation, *AtNRT2.5* becomes the most abundant transcript amongst the seven *AtNRT2* members in *Arabidopsis* shoots and roots [25]. Subsequent studies have revealed that *AtNRT3.1* and *AtNRT2.5* form a complex on the plasma membrane; this complex is a major contributor to high-affinity  $\text{NO}_3^-$  influx in *Arabidopsis* [17]. However, in our study, the *AtNRT3.1* expression in transformed seedlings was not altered (Figure 8). Thus, our results suggest that the heterologous expression of *DsNRT3.1* may enhance the  $\text{NO}_3^-$  uptake by affecting *AtNRT2.5* function, thereby affecting the seedling growth in *Arabidopsis* under N-starvation. To further elucidate the role and function of *DsNRT3.1*, future research should address the following aspects: (i) whether the heterologous expression of *DsNRT3.1* complements the function of the *atnrt3.1* mutant; and (ii) whether *DsNRT3.1* interacts with *AtNRT2* members, and particularly with *AtNRT2.5*, on the plasma membrane. Furthermore, we found that in the absence of  $\text{NO}_3^-$ , the root hairs of N-starved transformed *Arabidopsis* seedlings showed a stronger  $\text{NH}_4^+$  influx than those of the wild type (Figure 6G,H and Figure 7G,H), suggesting that the heterologous expression of *DsNRT3.1* may directly or indirectly affect the  $\text{NH}_4^+$  uptake under N-starvation. However, this requires further study. Recent studies have shown that *AtNRT1.1* participates in the  $\text{NH}_4^+$  uptake by affecting the  $\text{NH}_4^+$  transporter expression [26].

## 4. Materials and Methods

### 4.1. Sequence Analysis of *DsNRT3.1*

The amino acid sequence of *DsNRT3.1* (GenBank accession No. MN334698) and its homologs were aligned using BioEdit (<https://bioedit.software.informer.com/>). The phylogenetic tree was constructed using molecular evolutionary genetics analysis (MEGA) 4.1 software (available online: <http://www.megasoftware.net/>). The transmembrane domains prediction of *DsNRT3.1* was performed using the HMMTOP (<http://www.sacs.ucsf.edu/cgi-bin/hmmtop.py/>) software.

### 4.2. Plant Materials and Growth Conditions

Seeds of *D. spiculifolius* and *A. thaliana* (Columbia-0) were surface sterilized using 30% (*v/v*) bleach solution for 6 min and rinsed five times with sterile water. The sterilized seeds were grown on 1/2 strength Murashige and Skoog (MS) medium (10.3 mM  $\text{NH}_4\text{NO}_3$ , 9.4 mM  $\text{KNO}_3$ , 0.6 mM  $\text{KH}_2\text{PO}_4$ , 0.8 mM  $\text{MgSO}_4$ , 1.5 mM  $\text{CaCl}_2$ , 2.5  $\mu\text{M}$  KI, 50  $\mu\text{M}$   $\text{MnSO}_4$ , 50  $\mu\text{M}$   $\text{H}_3\text{BO}_3$ , 15  $\mu\text{M}$   $\text{ZnSO}_4$ , 0.5  $\mu\text{M}$   $\text{Na}_2\text{MoO}_4$ , 0.05  $\mu\text{M}$   $\text{CuSO}_4$ , 0.06  $\mu\text{M}$   $\text{CoCl}_2$ , 0.1 mM  $\text{FeSO}_4$ , 0.1 mM  $\text{Na}_2\text{-EDTA}$ ) medium supplemented with 1% agar and 3% sucrose (pH 5.8) under a 12 h light/12 h dark photoperiod (100  $\mu\text{mol m}^{-2} \text{s}^{-1}$  light intensity) at 22 °C.

For the different N-source treatments, *D. spiculifolius* seedlings were N-starved for 1 week, then transferred to N-free 1/2 MS medium (3% sucrose, 1% agar, pH 5.8) supplemented with 1 mM  $\text{KNO}_3$ , 1 mM KCl, 1 mM  $\text{NH}_4\text{NO}_3$ , or 0.5 mM  $(\text{NH}_4)_2\text{SO}_4$  as the sole N source. At least 10 seedlings from each treatment were harvested and pooled at different time points (0, 3, 6, 12, or 24 h after treatments), frozen immediately in liquid N, and stored at  $-80^\circ\text{C}$  for RNA preparation.

### 4.3. RNA Preparation and Expression Analysis

The total RNA (1.2  $\mu\text{g}$ ) was extracted using an RNeasy<sup>®</sup> Mini Kit (Qiagen, Valencia, CA, USA), and cDNA (20  $\mu\text{L}$ ) was synthesized using an M-MLV RTase cDNA Synthesis Kit (TaKaRa, Shiga, Japan), according to the manufacturers' instructions. The qPCR analysis was performed using Bio-Rad CFX Manager Software Version 3.1 (Bio-Rad, Hercules, CA, USA) using the appropriate pairs of species-specific primers (Supplementary Materials Table S1). The reaction components per 20  $\mu\text{L}$

were as follows: 7  $\mu$ L H<sub>2</sub>O, 10  $\mu$ L Hieff qPCR SYBR Green Master Mix (YEASEN, Shanghai, China), 1  $\mu$ L 10  $\mu$ M of each primer and 1  $\mu$ L cDNA. The thermal cycling program was as follows: initial denaturation at 95 °C for 60 s, and 40 cycles at 95 °C for 10 s, 60 °C for 30 s, and 72 °C for 30 s. *DsActin* or *AtActin* was used as an internal reference gene. The relative quantification of gene expression was evaluated using the delta-delta-Ct method. Three biological replicates and three technical replicates were performed for each analysis.

#### 4.4. Vector Construction and Plant Transformation

The open reading frame of *DsNRT3.1* was constructed into the pBI121 vector driven by 35S promoter, using the following restriction sites: 121DsNRT3.1(X)-F (TCTAGAAATGGCGGTGCGAGG ATTAAC; the XbaI site is underlined) and 121DsNRT3.1(S)-R (GAGCTCGCTAGCTAGCTTCCGACTT CTTC; the SacI site is underlined). To construct the *DsNRT3.1*-GFP fusion gene, the open reading frame of *DsNRT3.1* without a stop codon was constructed into a pBI121-GFP vector using the 121DsNRT3.1(X)-F and 121DsNRT3.1(K)-R (GGTACCGCTAGCTTCCGACTTCTTC; the KpnI site is underlined) restriction sites. These pBI121-GFP constructs have been described elsewhere [27]. These constructs were transformed into the *Agrobacterium tumefaciens* strain EHA105 for plant transformation; *Arabidopsis* was transformed using the floral dip method [28]. The transformed plants were placed on 1/2 MS medium containing 30  $\mu$ g mL<sup>-1</sup> kanamycin. The primers used in this study are shown in Supplementary Materials Table S1.

#### 4.5. Subcellular Localization of *DsNRT3.1*

Four-day-old seedlings grown on vertical 1/2 MS medium plates (0.5% sucrose, pH 5.8) were placed at room temperature. The roots of transformed *Arabidopsis* seedlings were re-washed using liquid 1/2 MS medium immediately before confocal laser scanning microscopy (CLSM) (Nikon, A1, Tokyo, Japan).

#### 4.6. Phenotypic Analysis of Transformed *Arabidopsis*

The sterilized wild-type and transformed *Arabidopsis* seeds were stratified for 3 days at 4 °C. The seedlings were then transferred to N-free 1/2 MS medium (3% sucrose, 1% agar, pH 5.8) supplemented with different concentrations of KNO<sub>3</sub> or NH<sub>4</sub>Cl (0, 0.01, 0.02, 0.05, 0.1, 0.3, 0.5, 1, or 2.5 mM) for 10 days before measuring root length, or 20 days before measuring the seedlings fresh weight. After examining seedling growth phenotypes, the plants were photographed using a Canon EOS 80D camera (Canon, Tokyo, Japan). Images were processed using Adobe Photoshop CS. Seedling root length was measured using Image Pro Plus 6.0 software (Media Cybernetics, Silver Spring, MD, USA). The fresh weight of the aerial parts of the seedlings was measured using an analytical balance with an accuracy of  $\pm$  0.1 mg.

#### 4.7. NMT Measurement of Net NO<sub>3</sub><sup>-</sup> and NH<sub>4</sub><sup>+</sup> Fluxes in *Arabidopsis* Root Hairs

The net fluxes of NO<sub>3</sub><sup>-</sup> and NH<sub>4</sub><sup>+</sup> in the root hairs of the wild-type and transformed *Arabidopsis* seedlings were measured using NMT (NMT100 Series, YoungerUSA LLC, Amherst, MA, USA) as previously described [29]. The wild-type and transformed *Arabidopsis* seeds were surface sterilized and kept at 4 °C for 3 days in the dark. After germination, the seedlings were transferred into N-free 1/2 MS medium for 7 days, after which the roots of the seedlings were immediately equilibrated in a measuring solution containing 0.1 mM KNO<sub>3</sub>, 0.1 mM NH<sub>4</sub>Cl, or 0.1 mM NH<sub>4</sub>NO<sub>3</sub> for 10 min. The roots were fixed to the bottom of the plate using resin blocks and filter paper strips. To take flux measurements, the ion-selective electrodes were calibrated using NO<sub>3</sub><sup>-</sup> or NH<sub>4</sub><sup>+</sup> at concentrations of 0.05 and 0.5 mM, respectively. The net fluxes of NO<sub>3</sub><sup>-</sup> or NH<sub>4</sub><sup>+</sup> in the root hairs were measured. Each sample was measured continuously for 10 min. The KNO<sub>3</sub> and NH<sub>4</sub>NO<sub>3</sub> measuring solution contained 0.1 mM KNO<sub>3</sub>, 0.1 mM CaCl<sub>2</sub>, 0.1 mM KCl, and 0.3 mM MES (pH 6.0). The NH<sub>4</sub>Cl measuring solution contained 0.1 mM NH<sub>4</sub>Cl, 0.1 mM CaCl<sub>2</sub>, and 0.3 mM MES (pH 6.0). The KNO<sub>3</sub> calibration solution

contained 0.5mM KNO<sub>3</sub>, 0.1 mM KCl, 0.1 mM CaCl<sub>2</sub> and 0.3 mM MES (pH 6.0); 0.05 mM KNO<sub>3</sub>, 0.1 mM KCl, 0.1 mM CaCl<sub>2</sub>, and 0.3 mM MES (pH 6.0). The NH<sub>4</sub>Cl calibration solution contained 0.5 mM NH<sub>4</sub>Cl, 0.1 mM CaCl<sub>2</sub>, and 0.3 mM MES (pH 6.0); 0.05 mM NH<sub>4</sub>Cl, 0.1 mM CaCl<sub>2</sub>, and 0.3 mM MES (pH 6.0). The NH<sub>4</sub>NO<sub>3</sub> calibration solution contained 0.5 mM NH<sub>4</sub>NO<sub>3</sub>, 0.1 mM CaCl<sub>2</sub>, and 0.3 mM MES (pH 6.0); 0.05 mM NH<sub>4</sub>NO<sub>3</sub>, 0.1 mM CaCl<sub>2</sub>, and 0.3 mM MES (pH 6.0). The calibration slopes for NO<sub>3</sub><sup>-</sup> and NH<sub>4</sub><sup>+</sup> were -55.61 and 56.19 mV/decade, respectively. Six biological repeats were performed for each analysis.

#### 4.8. Statistical Analysis

The data were analyzed using a one-way analysis of variance in SPSS (SPSS, Inc., Chicago, IL, USA), and statistically significant differences were calculated using the Student's *t*-test, with *p* < 0.05 as the threshold for significance.

### 5. Conclusions

In this study, the nitrate assimilation-related protein DsNAR2.1/DsNRT3.1 was characterized from *D. spiculifolius*. DsNRT3.1 was localized mainly in the plasma membrane of *Arabidopsis* root hair cells. The findings reveal that the heterologous expression of *DsNRT3.1* in *Arabidopsis* affects seedling root growth and NO<sub>3</sub><sup>-</sup> and NH<sub>4</sub><sup>+</sup> uptake under N-starvation, as well as the expression of *AtNRT2* family members. Overall, our results suggest that DsNRT3.1 may affect the seedling growth in N-starved *Arabidopsis* by enhancing the NO<sub>3</sub><sup>-</sup> and NH<sub>4</sub><sup>+</sup> uptake, which may be associated with altered *AtNRT2* family expression. Our study also suggests that DsNRT3.1 functions as a positive regulator of plant N uptake and could be utilized for the genetic improvement of N-efficient plants.

**Supplementary Materials:** The following are available online at <http://www.mdpi.com/1422-0067/21/11/4027/s1>, Table S1: List of PCR primers.

**Author Contributions:** Conceptualization, J.W. and A.Z.; investigation, H.M., J.Z. and A.Z.; resources, S.G., J.W. and A.Z.; data curation, S.F., K.Q. and S.G.; writing—original draft preparation, H.M. and A.Z.; writing—review and editing, H.M. and A.Z.; funding acquisition, S.G., J.W. and A.Z. All authors have read and agreed to the published version of the manuscript.

**Funding:** This study was supported by the National Natural Science Foundation of China (Nos. 31902052 and 31972450), the Natural Science Foundation of Heilongjiang Province of China (No. C2018021), and the 'Academic Backbone' Project of Northeast Agricultural University of China (No. 18XG08).

**Conflicts of Interest:** The authors declare no conflict of interest.

### References

1. Xu, G.H.; Fan, X.R.; Miller, A.J. Plant nitrogen assimilation and use efficiency. *Annu. Rev. Plant Biol.* **2012**, *63*, 153–182. [[CrossRef](#)] [[PubMed](#)]
2. Hachiya, T.; Sakakibara, H. Interactions between nitrate and ammonium in their uptake, allocation, assimilation, and signaling in plants. *J. Exp. Bot.* **2017**, *68*, 2501–2512. [[CrossRef](#)] [[PubMed](#)]
3. Wang, Y.Y.; Cheng, Y.H.; Chen, K.E.; Tsay, Y.F. Nitrate transport, signaling, and use efficiency. *Annu. Rev. Plant Biol.* **2018**, *69*, 85–122. [[CrossRef](#)] [[PubMed](#)]
4. Gao, Y.X.; Li, Y.; Yang, X.X.; Li, H.J.; Shen, Q.R.; Guo, S.W. Ammonium nutrition increases water absorption in rice seedlings (*Oryza sativa* L.) under water stress. *Plant Soil* **2010**, *331*, 193–201. [[CrossRef](#)]
5. Ruan, L.; Wei, K.; Wang, L.Y.; Cheng, H.; Zhang, F.; Wu, L.Y.; Bai, P.X.; Zhang, C.C. Characteristics of NH<sub>4</sub><sup>+</sup> and NO<sub>3</sub><sup>-</sup> fluxes in tea (*Camellia sinensis*) roots measured by scanning ion-selective electrode technique. *Sci. Rep.* **2016**, *6*, 38370. [[CrossRef](#)] [[PubMed](#)]
6. Fan, X.; Naz, M.; Fan, X.; Xuan, W.; Miller, A.J.; Xu, G. Plant nitrate transporters: From gene function to application. *J. Exp. Bot.* **2017**, *68*, 2463–2475. [[CrossRef](#)]
7. O'Brien, J.A.; Vega, A.; Bouguyon, E.; Krouk, G.; Gojon, A.; Coruzzi, G.; Gutierrez, R.A. Nitrate transport, sensing, and responses in plants. *Mol. Plant* **2016**, *9*, 837–856. [[CrossRef](#)]

8. Leran, S.; Varala, K.; Boyer, J.C.; Chiurazzi, M.; Crawford, N.; Daniel-Vedele, F.; David, L.; Dickstein, R.; Fernandez, E.; Forde, B.; et al. A unified nomenclature of NITRATE TRANSPORTER 1/PEPTIDE TRANSPORTER family members in plants. *Trends Plant Sci.* **2014**, *19*, 5–9. [\[CrossRef\]](#)
9. Von Wittgenstein, N.J.; Le, C.H.; Hawkins, B.J.; Ehrling, J. Evolutionary classification of ammonium, nitrate, and peptide transporters in land plants. *BMC Evol. Biol.* **2014**, *14*, 11. [\[CrossRef\]](#)
10. Wang, Y.Y.; Hsu, P.K.; Tsay, Y.F. Uptake, allocation and signaling of nitrate. *Trends Plant Sci.* **2012**, *17*, 458–467. [\[CrossRef\]](#)
11. Miller, A.J.; Fan, X.R.; Orsel, M.; Smith, S.J.; Wells, D.M. Nitrate transport and signalling. *J. Exp. Bot.* **2007**, *58*, 2297–2306. [\[CrossRef\]](#)
12. Feng, H.; Yan, M.; Fan, X.; Li, B.; Shen, Q.; Miller, A.J.; Xu, G. Spatial expression and regulation of rice high-affinity nitrate transporters by nitrogen and carbon status. *J. Exp. Bot.* **2011**, *62*, 2319–2332. [\[CrossRef\]](#)
13. Quesada, A.; Galvan, A.; Fernandez, E. Identification of nitrate transporter genes in *Chlamydomonas reinhardtii*. *Plant J.* **1994**, *5*, 407–419. [\[CrossRef\]](#)
14. Yong, Z.; Kotur, Z.; Glass, A.D. Characterization of an intact two-component high-affinity nitrate transporter from Arabidopsis roots. *Plant J.* **2010**, *63*, 739–748. [\[CrossRef\]](#)
15. Kotur, Z.; Mackenzie, N.; Ramesh, S.; Tyerman, S.D.; Kaiser, B.N.; Glass, A.D. Nitrate transport capacity of the *Arabidopsis thaliana* NRT2 family members and their interactions with AtNAR2.1. *New Phytol.* **2012**, *194*, 724–731. [\[CrossRef\]](#)
16. Okamoto, M.; Kumar, A.; Li, W.; Wang, Y.; Siddiqi, M.Y.; Crawford, N.M.; Glass, A.D. High-affinity nitrate transport in roots of Arabidopsis depends on expression of the NAR2-like gene AtNRT3.1. *Plant Physiol.* **2006**, *140*, 1036–1046. [\[CrossRef\]](#)
17. Kotur, Z.; Glass, A.D. A 150 kDa plasma membrane complex of AtNRT2.5 and AtNAR2.1 is the major contributor to constitutive high-affinity nitrate influx in *Arabidopsis thaliana*. *Plant Cell Environ.* **2015**, *38*, 1490–1502. [\[CrossRef\]](#)
18. Yan, M.; Fan, X.; Feng, H.; Miller, A.J.; Shen, Q.; Xu, G. Rice OsNAR2.1 interacts with OsNRT2.1, OsNRT2.2 and OsNRT2.3a nitrate transporters to provide uptake over high and low concentration ranges. *Plant Cell Environ.* **2011**, *34*, 1360–1372. [\[CrossRef\]](#)
19. Liu, X.; Huang, D.; Tao, J.; Miller, A.J.; Fan, X.; Xu, G. Identification and functional assay of the interaction motifs in the partner protein OsNAR2.1 of the two-component system for high-affinity nitrate transport. *New Phytol.* **2014**, *204*, 74–80. [\[CrossRef\]](#)
20. Zhou, A.; Ma, H.; Liu, E.; Jiang, T.; Feng, S.; Gong, S.; Wang, J. Transcriptome sequencing of *Dianthus spiculifolius* and analysis of the genes involved in responses to combined cold and drought stress. *Int. J. Mol. Sci.* **2017**, *18*, 849. [\[CrossRef\]](#)
21. Bohme, K.; Li, Y.; Charlot, F.; Grierson, C.; Marrocco, K.; Okada, K.; Laloue, M.; Nogue, F. The Arabidopsis COW1 gene encodes a phosphatidylinositol transfer protein essential for root hair tip growth. *Plant J.* **2004**, *40*, 686–698. [\[CrossRef\]](#)
22. Tong, Y.; Zhou, J.J.; Li, Z.; Miller, A.J. A two-component high-affinity nitrate uptake system in barley. *Plant J.* **2005**, *41*, 442–450. [\[CrossRef\]](#)
23. Gu, C.; Zhang, X.; Jiang, J.; Guan, Z.; Zhao, S.; Fang, W.; Liao, Y.; Chen, S.; Chen, F. Chrysanthemum CmNAR2 interacts with CmNRT2 in the control of nitrate uptake. *Sci. Rep.* **2014**, *4*, 5833. [\[CrossRef\]](#)
24. Li, H.; Yu, M.; Du, X.Q.; Wang, Z.F.; Wu, W.H.; Quintero, F.J.; Jin, X.H.; Li, H.D.; Wang, Y. NRT1.5/NPF7.3 functions as a proton-coupled H<sup>+</sup>/K<sup>+</sup> antiporter for K<sup>+</sup> loading into the xylem in Arabidopsis. *Plant Cell* **2017**, *29*, 2016–2026. [\[CrossRef\]](#)
25. Lezhneva, L.; Kiba, T.; Feria-Bourrellier, A.B.; Lafouge, F.; Boutet-Mercey, S.; Zoufan, P.; Sakakibara, H.; Daniel-Vedele, F.; Krapp, A. The Arabidopsis nitrate transporter NRT2.5 plays a role in nitrate acquisition and remobilization in nitrogen-starved plants. *Plant J.* **2014**, *80*, 230–241. [\[CrossRef\]](#)
26. Jian, S.; Liao, Q.; Song, H.; Liu, Q.; Lepo, J.E.; Guan, C.; Zhang, J.; Ismail, A.M.; Zhang, Z. NRT1.1-related NH<sub>4</sub><sup>+</sup> toxicity is associated with a disturbed balance between NH<sub>4</sub><sup>+</sup> uptake and assimilation. *Plant Physiol.* **2018**, *178*, 1473–1488. [\[CrossRef\]](#)
27. Zhou, A.; Bu, Y.; Takano, T.; Zhang, X.; Liu, S. Conserved V-ATPase c subunit plays a role in plant growth by influencing V-ATPase-dependent endosomal trafficking. *Plant Biotechnol. J.* **2016**, *14*, 271–283. [\[CrossRef\]](#)

28. Clough, S.J.; Bent, A.F. Floral dip: A simplified method for *Agrobacterium*-mediated transformation of *Arabidopsis thaliana*. *Plant J.* **1998**, *16*, 735–743. [[CrossRef](#)]
29. Bai, L.; Ma, X.; Zhang, G.; Song, S.; Zhou, Y.; Gao, L.; Miao, Y.; Song, C.P. A receptor-like kinase mediates ammonium homeostasis and is important for the polar growth of root hairs in *Arabidopsis*. *Plant Cell* **2014**, *26*, 1497–1511. [[CrossRef](#)]



© 2020 by the authors. Licensee MDPI, Basel, Switzerland. This article is an open access article distributed under the terms and conditions of the Creative Commons Attribution (CC BY) license (<http://creativecommons.org/licenses/by/4.0/>).